IEICE TRANS. ELECTRON., VOL.E89–C, NO.10 OCTOBER 2006

INVITED PAPER *Special Section on Electronic Displays*

New Silicate Phosphors for a White LED

Kenji TODA[†a)], **Yoshitaka KAWAKAMI**[††], **Shin-ichiro KOUSAKA**[††], **Yutaka ITO**[†], **Akira KOMENO**[†], **Kazuyoshi UEMATSU**[††], ***and*** **Mineo SATO**[††], ***Nonmembers***

SUMMARY We focus on the development of new silicate phosphors for a white LED. In the europium doped silicate system, four LED phosphor candidates—$Li_2SrSiO_4:Eu^{2+}$, $Ba_9Sc_2Si_6O_{24}:Eu^{2+}$, $Ca_3Si_2O_7:Eu^{2+}$ and $Ba_2MgSi_2O_7:Eu^{2+}$ were found. Luminescent properties under near UV and visible excitation were investigated for the new Eu^{2+} doped LED silicate phosphors. These new phosphors have a relatively strong absorption band in a long wavelength region.

key words: *phosphor, silicate, white LED*

1. Introduction

The Hg-discharge fluorescent lamp illuminates around us and helps our comfortable life. After July 2006, RoHS directive restricts the use of hazardous substances such as Pb, Hg and Cd in the manufacture of electrical and electronic equipment. Therefore, the electrical and electronic equipment containing such harmful materials can not be introduced to the European market. Although the Hg-discharge based fluorescent lamps were not the restriction object at present, the Hg based lighting will be prohibited in the near future.

White LED is one of the possible candidates for new lighting system in the near future. There are three important structures for a single chip white LED. The most dominant white LED use a 450–470 nm blue-emitting LED that excites a yellow-emitting $Y_3Al_5O_{12}:Ce^{3+}$ ($YAG:Ce^{3+}$) phosphor dispersed in the epoxy resin on a blue LED chip [1]. This method is presently the most efficient technique. However, the light color is not true white (lack of red component). Therefore, the importance of blue-excitable red-emitting phosphor is increasing. The second method is to combine a blue LED with the blue-excitable red and green phosphors. The third option is to set three-phosphors (red, green and blue) on the UV-emitting LED.

Customers require new phosphors that offer good color and durability at low cost for the white LED. Silicate phosphors are most attractive candidates for the white LED applications. In this paper, we report the synthesis and luminescence properties of four new silicate phosphors for blue LED based white LEDs.

Manuscript received April 14, 2006.
Manuscript revised July 4, 2006.

[†]The authors are with Graduate School of Science and Technology, Niigata University, Niigata-shi, 950-2181 Japan.
[††]The authors are with the Faculty of Engineering, Niigata University, Niigata-shi, 950-2181 Japan.
a) E-mail: ktoda@eng.niigata-u.ac.jp

DOI: 10.1093/ietele/e89–c.10.1406

In these phosphors, the blue light can be strongly absorbed by the allowed f-d transition of Eu^{2+}. The emissions at about 580 nm ($Li_2SrSiO_4:Eu^{2+}$), 500–520 nm ($Ba_9Sc_2Si_6O_{24}:Eu^{2+}$), 600 nm ($Ca_3Si_2O_7:Eu^{2+}$) and 505 nm ($Ba_2MgSi_2O_7:Eu^{2+}$) depends on the environment of the emission ion site in the host lattice. New silicate phosphors have relatively strong and rigid characteristics of partly covalent Si-O bond. In addition, rigid frameworks often provide relatively distorted coordination around the emission ion. Therefore, strong crystal fields were observed in many silicate phosphors. Although quantitative predictions of the f-d emission wavelength are difficult for various kinds of phosphors, effects of asymmetrical coordination environments for the emission wavelength are well known [2]–[4]. Strong crystal fields with the covalent bond and distorted coordination affect the excited state because the energy level of the $4f^65d$ has a wide distribution of the electron cloud. Since the splitting of $4f^65d$ energy level becomes wider with the increase of the crystal field strength, the difference between the ground state ^8S level and lower $4f^65d$ component becomes smaller. Therefore, the luminescence wavelength shifts to long wavelength side.

Nitride red emitting phosphors such as Eu^{2+} doped $Ba_2Si_5O_8$ [5] and $CaAlSiN_3$ [6] also have the covalent bond and distorted coordination. The new LED silicate phosphors were designed with a similar design philosophy (rigid framework and strong covalent matrix) of the nitride phosphors and attractive candidates for new blue-excitable phosphors for a white LED.

2. Experimental

Polycrystalline samples were synthesized using a conventional solid-state reaction. The starting material was a stoichiometric mixture of high purity carbonates and oxides. Powder X-ray diffraction (XRD) data were obtained using a diffractometer (MX-Labo; Mac Science Ltd.). Simulations of the XRD patterns were carried out with a software FindIt on Inorganic Crystal Structure Database (Fachinformationzentrum Karlsruhe). Powder neutron diffraction patterns were recorded using the HERMES(T1-3) diffractometer installed at JRR-3M Guide Hall in the Japan Atomic Energy Research Institute (JAERI) [7]. The powder XRD and neutron patterns obtained were analyzed using the RIETAN2000 profile refinement program [8].

Excitation and emission spectra in the UV range were

measured for the powder sample using a spectrofluorometer (FP-6500/6600; Jasco Inc.). Temperature dependences of photoluminescence were measured from by 300 to 473 K with a 11 W black light (365 nm) as an excitation source and with Photonic Multichannel Spectral Analyzer (PMA-11; Hamamatsu Corporation) powder samples in a cryostat equipped with a temperature controller.

3. Results and Discussion

3.1 Li_2SrSiO_4

A stoichiometric mixture was fired in an alumina crusible at 1173 K for 12 h in air. The sample after firing was ground and fired in an alumina boat at 1173 K for 12 h under a weak reductive atmosphere of 5% H_2-95% Ar gas flow. Figure 1 shows XRD patterns of isotypic Li_2EuSiO_4 (simulation) and $Li_2Sr_{0.98}Eu_{0.02}SiO_4$. The crystal structure of Li_2SrSiO_4 is given in Fig. 2. The tetrahedral [LiO_4] and [SiO_4] are connected via common corners and build up a three-dimensional network for the space of Sr^{2+} (Eu^{2+}) ion with a distorted eightfold coordination. The crystal structure of $Li_2Sr_{0.98}Eu_{0.02}SiO_4$ determined by X-ray diffraction is $P3_121$, a = 0.5030(3) nm and c = 1.2470(5) nm, which is an isostructure with Li_2EuSiO_4 [9]. Figure 3 shows the Sr/Eu coordination environment of the Li_2SrSiO_4:Eu^{2+}. The site asymmetry leads to strong crystal fields. Figure 4 shows the excitation and emission spectra of $Li_2(Sr_{0.98}Eu_{0.02})SiO_4$. The phosphor can be efficiently excited by blue region of the visible light (400–480 nm), yielding a reddish yellow emission around 570 nm. The emission intensity of the phosphor is comparable to that of the YAG:Ce^{3+} phosphor. Figure 5 shows the temperature dependence of luminescence intensity. At 100°C, the decrease in emission intensity of $Li_2(Sr_{0.98}Eu_{0.02})SiO_4$ is only a 10 percent, indicating a weak thermal quenching behavior [10].

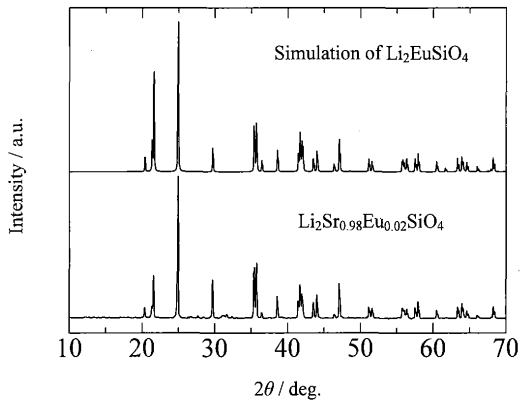

Fig. 1 Simulation XRD pattern of Li_2EuSiO_4 and experimental XRD pattern of $Li_2Sr_{0.98}Eu_{0.02}SiO_4$.

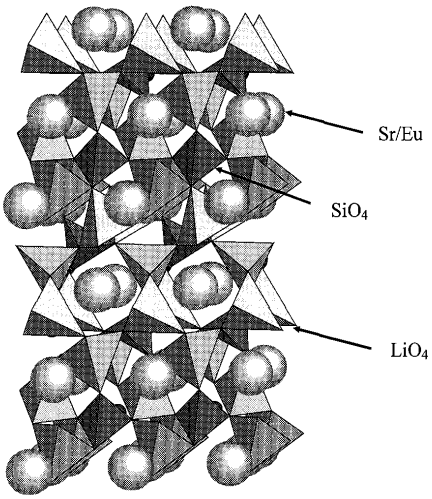

Fig. 2 Crystal structure of Li_2SrSiO_4.

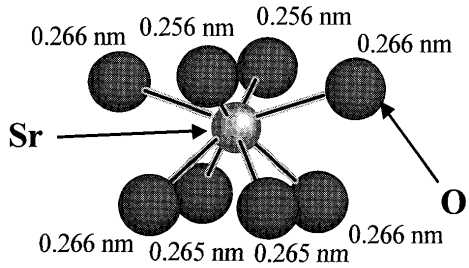

Fig. 3 Sr/Eu coordination environment of the Li_2SrSiO_4:Eu^{2+}.

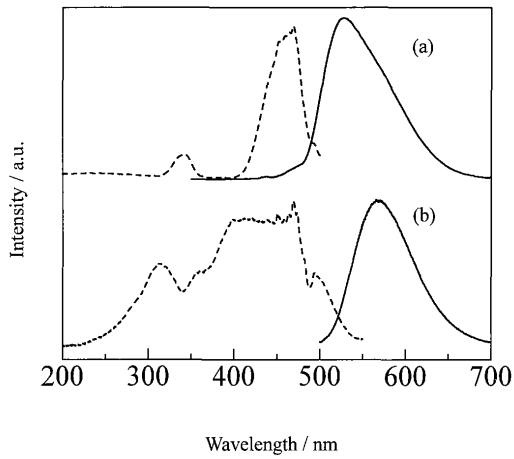

Fig. 4 Excitation and emission spectra of (a) YAG:Ce^{3+} and (b) $Li_2(Sr_{0.98}Eu_{0.02})SiO_4$.

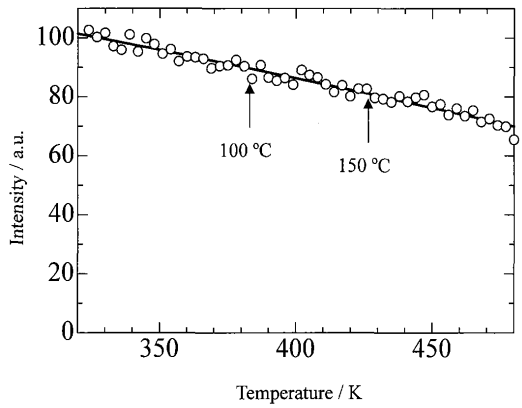

Fig. 5 Temperature dependence of emission intensity for $Li_2(Sr_{0.98}Eu_{0.02})SiO_4$.

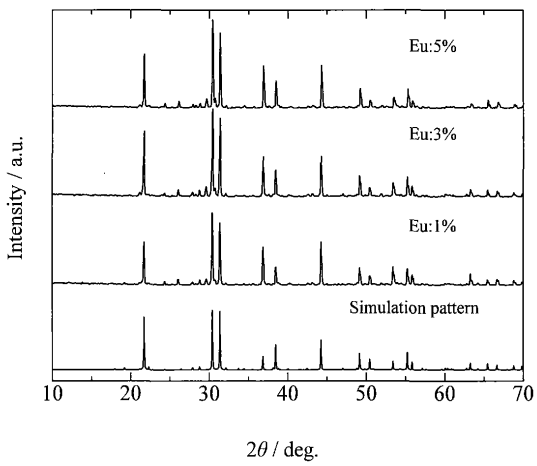

Fig. 6 XRD patterns of $Ba_9Sc_2Si_6O_{24}$ (simulation) and $(Ba_{1-x}Eu_x)_9Sc_2Si_6O_{24}$.

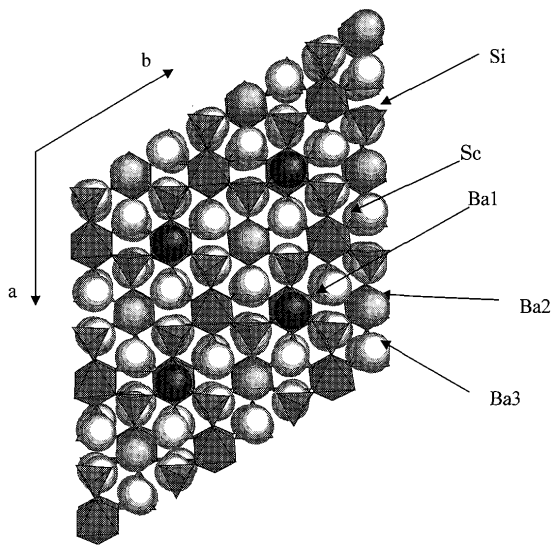

Fig. 7 Crystal structure of $Ba_9Sc_2Si_6O_{24}$.

3.2 $Ba_9Sc_2Si_6O_{24}$

A stoichiometric mixture was fired in an alumina boat at 1773 K for 6 h in weak reductive atmosphere of 5% H_2-95% Ar gas. Figure 6 shows XRD patterns of $Ba_9Sc_2Si_6O_{24}$ (simulation) and $(Ba_{1-x}Eu_x)_9Sc_2Si_6O_{24}$. The crystal structure of $Ba_9Sc_2Si_6O_{24}$ is given in Fig. 7 [11]. The structure closely resembles the structure of NASICON in their linkage of $[SiO_4]$ tetrahedral and $[ScO_6]$ octahedral [12]. Figures 8–10 show the Ba sites in $Ba_9Sc_2Si_6O_{24}$. There are three different Ba sites. The coordinations of the Ba^{2+} are slightly irregular nine-, ten- and twelve-folds. Figure 11 shows the excitation and emission spectra of $(Ba_{1-x}Eu_x)_9Sc_2Si_6O_{24}$ at room temperature. The phosphor can be efficiently excited by visible lights (350–450 nm), yielding an intense green emission around 510 nm. The emission intensity is comparable to that of the commercial YAG:Ce^{3+} phosphor. At 100°C, the decrease in emission intensity is a 25 percent.

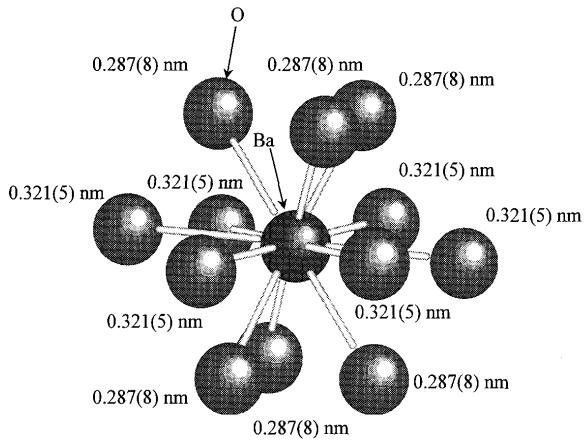

Fig. 8 Ba(1) site in $Ba_9Sc_2Si_6O_{24}$.

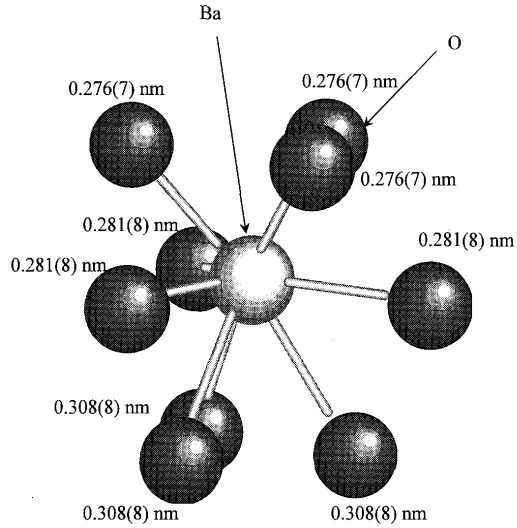

Fig. 9 Ba(2) site in $Ba_9Sc_2Si_6O_{24}$.

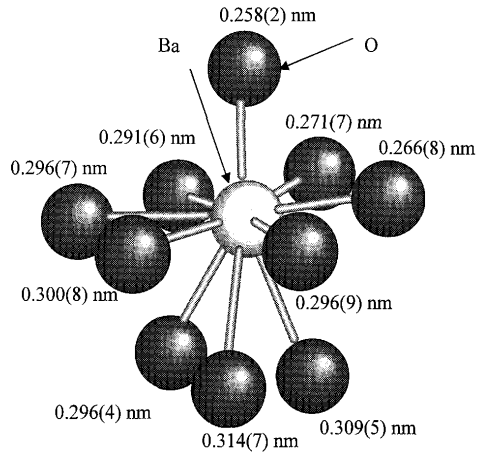

Fig. 10 Ba(3) site in $Ba_9Sc_2Si_6O_{24}$.

3.3 $Ca_3Si_2O_7$

A stoichiometric mixture was fired in an alumina crusible at 1573 K for 6 h in air. The samples after firing was ground and fired in an alumina boat at 1573 K for 6 h under

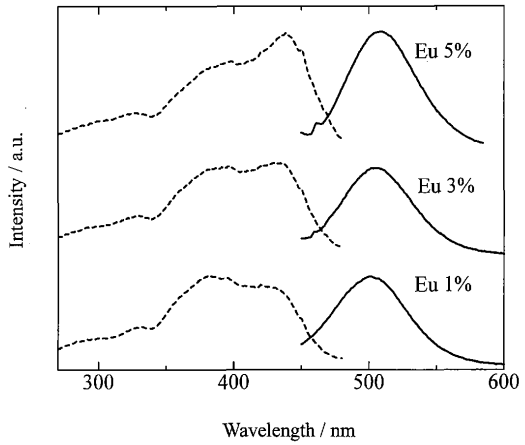

Fig. 11 Excitation and emission spectra of $Ba_9Sc_2Si_6O_{24}$.

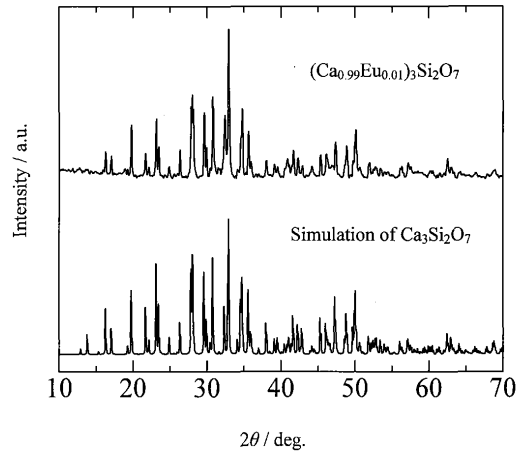

Fig. 12 XRD patterns of $Ca_3Si_2O_7$ (simulation) and $(Ca_{0.99}Eu_{0.01})_3Si_2O_7$.

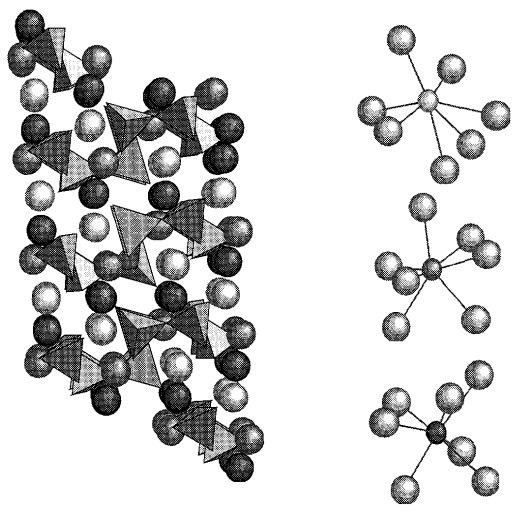

Fig. 13 Crystal structure of $Ca_3Si_2O_7$.

a weak reductive atmosphere of 5% H_2-95% Ar gas. Figure 12 shows XRD patterns of $Ca_3Si_2O_7$ (simulation) and $(Ca_{0.99}Eu_{0.01})_3Si_2O_7$. The crystal structure of $Ca_3Si_2O_7$ is shown in Fig. 13 [13]. Three crystallographically different coordination polyhedra of Ca ions form two dimensional

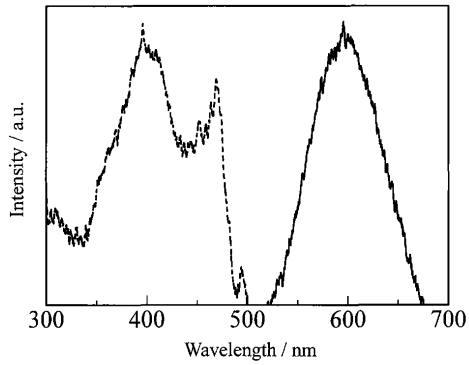

Fig. 14 Excitation and emission spectra of $(Ca_{0.99}Eu_{0.01})_3Si_2O_7$.

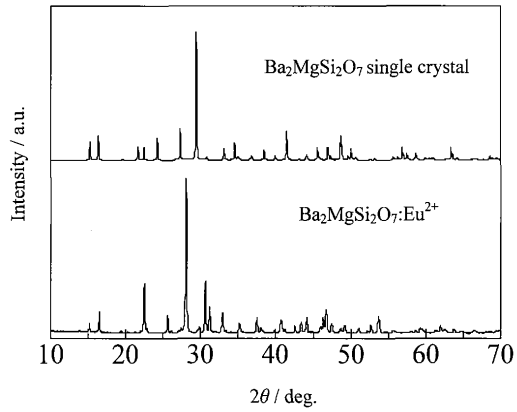

Fig. 15 XRD patterns of $Ba_2MgSi_2O_7$ single crystal (simulation pattern) and $Ba_2MgSi_2O_7$:Eu^{2+} sample.

sheets between $[Si_2O_7]$ groups. The coordinations of the Ca^{2+} sites are extremely irregular seven-folds. The bond distances of Ca-O range from 0.230 to 0.289 nm.

Figure 14 shows the excitation and emission spectra of $(Ca_{0.99}Eu_{0.01})_3Si_2O_7$. Broad excitation band extending to 470 nm can be observed. The phosphor emits orangish red light at about 600 nm. It is well known that the emission wavelength of Eu^{2+} range from red to UV depending on the crystal structure of host material [14]. In most silicates, the emission of Eu^{2+} center lies in the range between the near UV and green. The long wavelength emission of $Ca_3Si_2O_7$:Eu^{2+} results from the strong crystal filed by the distorted coordination environments of emission centers.

3.4 $Ba_2MgSi_2O_7$

A stoichiometric mixture was fired in an alumina crusible at 1523 K for 6 h in air. The sample after firing was ground and fired in an alumina boat at 1523 K for 6 h under a weak reductive atmosphere of 5% H_2-95% Ar gas flow. M. Shimizu et al. reported that the crystal structure of $Ba_2MgSi_2O_7$ was an akermanite-type structure with the tetragonal space group from single crystal X-ray investigation [15]. However, the powder XRD pattern of $(Ba_{0.95}Eu_{0.05})_2MgSi_2O_7$ differs from the simulation pattern of single crystal $Ba_2MgSi_2O_7$. A comparison between the powder and single crystal XRD patterns is shown in Fig. 15. The crystal structure of un-

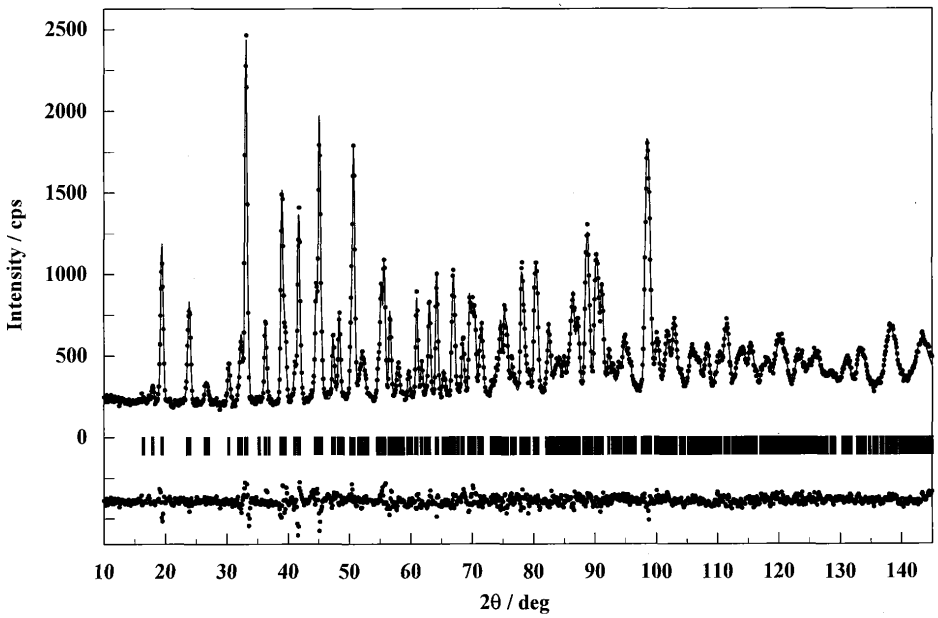

Fig. 16 Neutron pattern fitting of $Ba_2MgSi_2O_7$. The calculated and observed patterns are shown on the top solid line and the dots, respectively. The vertical marks in the middle show positions calculated for Bragg reflections. The trace on the bottom is a plot of the difference between calculated and observed intensities.

Table 1 Crystallographic data of the monoclinic $Ba_2MgSi_2O_7$.

Atoms	Site	g	x	y	z	B / nm^2
Ba	8f	1	0.272(5)	0.044(1)	0.476(1)	0.0084(4)
Mg	4e	1	0.0	0.744(1)	0.25	0.009(2)
Si	8f	1	0.111(1)	0.282(5)	0.133(1)	0.007(1)
O1	8f	1	0.100(1)	0.142(1)	0.120(2)	0.015(3)
O2	8f	1	0.303(1)	0.342(1)	0.235(1)	0.003(1)
O3	8f	1	0.479(1)	0.149(1)	0.042(1)	0.001(4)
O4	4e	1	0.0	0.334(1)	0.25	0.009(4)

Space group : C 2/c (A-15)

Lattice parameter a = 0.8425(8) nm, b = 1.0732(8) nm, c = 0.8454(8) nm, β = 110.723(5)°

Rwp = 5.65 % Rp = 4.34 % RR = 9.84 % Re = 4.57 % S = 1.23

doped powder sample, $Ba_2MgSi_2O_7$, also differ from the tetragonal symmetry. According to the indexing of the XRD patterns for the powder samples, $Ba_2MgSi_2O_7$: Eu^{2+} and $Ba_2MgSi_2O_7$ have monoclinic symmetry, C2/c (No. 15). Pattern fitting and crystallographic data refined by the powder neutron diffraction of $Ba_2MgSi_2O_7$ are shown in Fig. 16 and Table 1. Refined crystallographic parameters of $Ba_2MgSi_2O_7$powder sample were: a = 0.8425 (8) nm, b = 1.0732(8) nm, c = 0.8454(8) nm, and β = 110.723(5)°. The crystal structure of $Ba_2MgSi_2O_7$ is shown in Fig. 17. The crystal structure is layered structure with the double Ba^{2+} ion layer between distorted layers consist of [SiO_4] and [MgO_4] tetrahedral. Figure 18 shows the coordination environment of Eu in the monoclinic $Ba_2MgSi_2O_7$. In the tetragonal $Ba_2MgSi_2O_7$, the barium ions are coordinated neighboring eight oxygens with the center symmetry. On the other hand, the Eu ions in the monoclinic $Ba_2MgSi_2O_7$

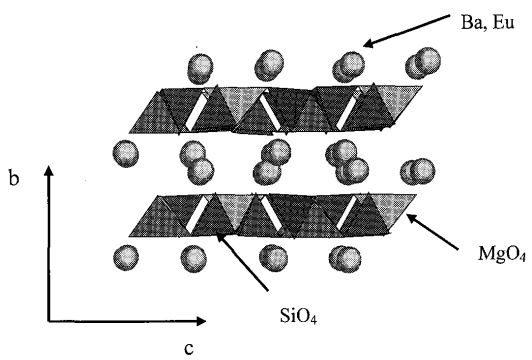

Fig. 17 Crystal structure of monoclinic $Ba_2MgSi_2O_7$.

have distorted coordination without the center symmetry. Figure 19 shows the excitation and emission spectra of $(Ba_{0.95}Eu_{0.05})_2MgSi_2O_7$ at room temperature. In general, Eu^{2+} doped-alkaline earth silicates show the tendency by

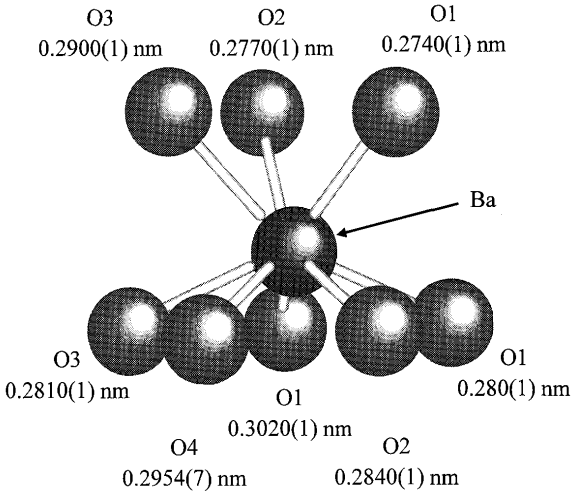

Fig. 18 The coordination environment of Eu in the monoclinic $Ba_2MgSi_2O_7$.

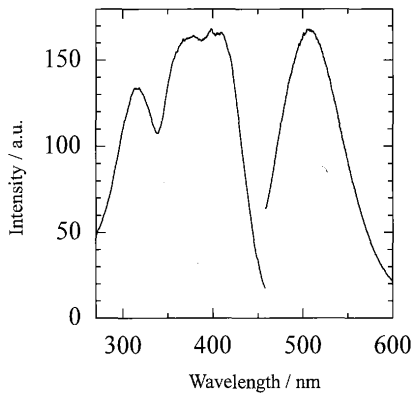

Fig. 19 Excitation and emission spectra of $(Ba_{0.95}Eu_{0.05})_2MgSi_2O_7$.

which the wavelength shifts to the longer wavelength side through substitution for smaller radius alkaline earth ions in a similar coordination environment [16]. On the contrast with the middle $Sr_2MgSi_2O_7$:Eu^{2+} (blue) and small $Ca_2MgSi_2O_7$:Eu^{2+} (yellow), monoclinic $(Ba_{0.95}Eu_{0.05})_2MgSi_2O_7$ emits green light at about 505 nm by the excitation of near-UV and blue lights (360–450 nm). The irregular shift of the luminescence wavelengths due to the crystal field influence of the asymmetric distorted coordination for the monoclinic $(Ba_{0.95}Eu_{0.05})_2MgSi_2O_7$. The emission intensity of $(Ba_{0.95}Eu_{0.05})_2MgSi_2O_7$ is comparable to that of the commercial YAG:Ce^{3+} phosphor. At 100°C, the decrease in emission intensity is a 15 percent, indicating a weak thermal quenching behavior.

4. Conclusion

We designed and synthesized the four novel silicate phosphors, Li_2SrSiO_4:Eu^{2+}, $Ba_9Sc_2Si_6O_{24}$:Eu^{2+}, $Ca_3Si_2O_7$:Eu^{2+} and $Ba_2MgSi_2O_7$:Eu^{2+}, for white LED application. These phosphors show characteristic luminescence properties depending on the host crystal structures. Common structural feature is an asymmetric distorted coordination for the Eu^{2+} ions. The network structures connected by partly covalent Si-O bond present the distorted space of the Eu^{2+} ions. The strong crystal fields contract the interval in the d orbital and the f orbital and emission wavelength shifts to the long-wavelength side.

In addition, the silicate phosphors can be prepared by a low-temperature process or cost-effective method without expensive precursors and equipment such as the nitride phosphors.

Acknowledgments

This research was supported by a Science and Technology Grant for Millennium Projects (No. 12317).

References

[1] Y.Q. Li, A.C.A. Delsing, G. de With, and H.T.J.M. Hintzen, "Luminescence properties of Eu^{2+}-Activated alkaline-earth silicon-oxynitride $MSi_2O_{2-\delta}N_{2+2/3\delta}$ (M = Ca, Sr, Ba): A promising class of novel LED conversion phosphors," Chem. Mater., vol.17, no.12, pp.3242–3248, 2005

[2] A. Diaz and D.A. Keszler, "Red, green, and blue Eu^{2+} luminescence in solid-state borates: A structure-property relationship," Materials Research Bulletin, vol.31, no.2, pp.147–151, 1996.

[3] A.L. Diaz and D.A. Keszler, "Eu^{2+} luminescence in the borates $X_2Z(BO_3)_2$ (X = Ba, Sr; Z = Mg, Ca)," Chem. Mater., vol.9, pp.2071–2077, 1997.

[4] P. Dorenbos, "Crystal field splitting of lanthanide $4f^{n-1}5d$-levels in inorganic compounds," J. Alloys Compd,, vol.341, no,1-2, pp.156–159, 2002.

[5] Y.Q. Li, J.E.J. van Steen, J.W.H. van Krevel, G. Botty, A.C.A. Delsing, F.J. DiSalvo, G. de With, and H.T.J.M. Hintzen, "Luminescence properties of red-emitting $M_2Si_5N_8$: Eu^{2+} (M = Ca, Sr, Ba) LED conversion phosphors," J. Alloys Compd., vol.417, no.1-2, pp.273–279, 2006.

[6] K. Uheda, H. Yamamoto, et al., "New red phosphor CaAlSiN3:Eu for white LEDs," Electrochemical and Solid-State Lett., vol.9, no.4, 2006.

[7] K. Ohoyama, T. Kanouchi, K. Nemoto, M. Ohashi, T. Kajitani, and Y. Yamaguchi, "The new neutron powder diffractometer with a multi-detector system for high-efficiency and high-resolution measurements," Jpn. J. Appl. Phys., vol.37, p.3319, 1998.

[8] F. Izumi and T. Ikeda, "A rietveld-analysis program RIETAN-98 and its applications to zeolites," Materials Science Forum, pp.321–324, 2000.

[9] B. Haferkorn and G. Meyer, Z. Anorg. Allg. Chem., vol.624, p.1079, 1998.

[10] Y. Umetsu, S. Okamoto, Y. Mita, and H. Yamamoto, Proc. 306th Meeting of Phosphor Research Society (The Electrochemical Society of Japan), p.23, 2005.

[11] L.H. Wang, L.F. Schneewexer, R.J. Cava, and T. Siegrist, "A new barium scandium silicate: $Ba_9Sc_2(SiO_4)_6$," J. Solid State Chem., vol.113, pp.211–214, 1994.

[12] Y. Hasegawa, S. Tamura, N. Imanaka, G. Adachi, Y. Takano, and K. Sekizawa, "Trivalent praseodymium ion conducting solid electrolyte composite with NASICON type structure," J. Alloys Compd., vol.375, pp.212–216, 2004.

[13] I. Kusachi, "The structure of rankinite," Mineralogical Journal, vol.8, pp.38–47, 1975.

[14] P. Dorenbos, "Energy of the first $4f^74f^65d$ transition of Eu^{2+} in inorganic compounds," J. Lumin., vol.104, pp.239–260, 2003.

[15] M. Shimizu, M. Kimata, and I. Iida, "Crystal structure of $Ba_2MgSi_2O_7$ melilite: The longest tetrahedral Mg-O distance," N. Jb. Miner. Mh., Jg. 1995, H. 1, 39, 1995.

[16] G. Blasse, W.L. Wanmaker, J.W. Ter Vrugt, and A. Bril, "Fluorescence of Eu^{2+}-activated silicates," Philips Research Reports, vol.23, no.2, pp.189–200, 1968.

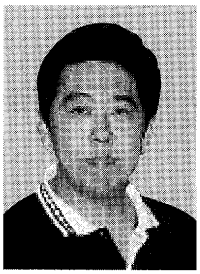

Kenji Toda received the Doctral degree from Niigata University in 1995. During 1988–1992, he stayed in Nippon Kodoshi Corporation. He now with Graduate School of Science and Technology, Niigata University (Associate Professor).

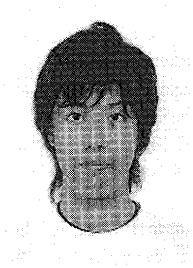

Yoshitaka Kawakami Master course student, Graduate School of Science and Technology, Niigata University.

Shin-ichiro Kousaka Master course student, Graduate School of Science and Technology, Niigata University.

Yutaka Ito Master course student, Graduate School of Science and Technology, Niigata University.

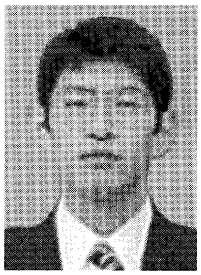

Akira Komeno Doctoral course student, Graduate School of Science and Technology, Niigata University.

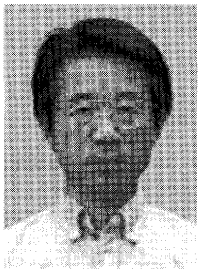

Kazuyoshi Uematsu Technical officer of Chemistry and Chemical Engineering, Faculty of Engineering, Niigata University.

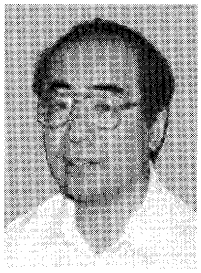

Mineo Sato received the Doctral degree from Osaka University in 1981. He now with Faculty of Engineering, Niigata University (Professor).